

AD 74249

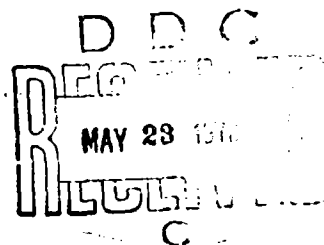
AFOSR - TR - 72 - 1125

## FINAL REPORT

Depressurization Extinguishment of Composite Solid Propellants:  
Flame Structure, Surface Characteristics, and Restart Capability.

Dec 1970

J.A. Stein z and H. S e l z e r



Deutsche Forschungs- und Versuchsanstalt für Luft- u. Raumfahrt e.V.  
( DFVR ), Institut für Chemische Raketenantriebe  
3041 Trauen, W. Germany

Reproduced from  
best available copy.

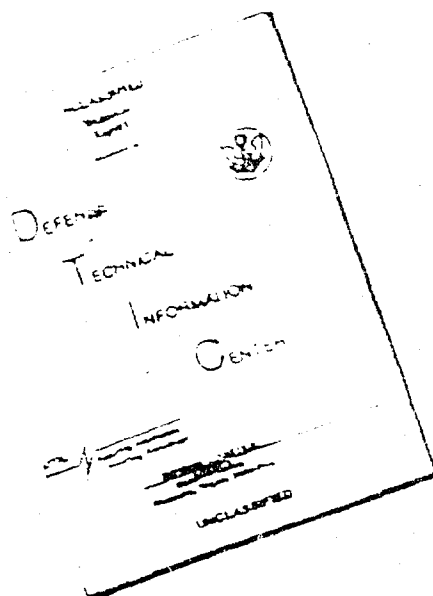
This research has been sponsored in part by Air Force Office of  
Scientific Research through the European Office of Aerospace  
Research, OAR, United States Air Force under Contract F01052-  
70-C-0013.

Reproduced by  
NATIONAL TECHNICAL  
INFORMATION SERVICE  
Springfield, Va. 22151

Approved for public release;  
distribution unlimited.

Supersedes AD-733588

# DISCLAIMER NOTICE



THIS DOCUMENT IS BEST  
QUALITY AVAILABLE. THE COPY  
FURNISHED TO DTIC CONTAINED  
A SIGNIFICANT NUMBER OF  
PAGES WHICH DO NOT  
REPRODUCE LEGIBLY.

REPRODUCED FROM  
BEST AVAILABLE COPY

Depressurization Extinguishment of Composite Solid Propellants:  
Flame Structure, Surface Characteristics, and Restart Capability\*

By

J.A. Steinz and H. Selzer<sup>†</sup>

ABSTRACT

During a rapid depressurization, the intensities of several spectral lines and the pressure are measured, simultaneous to the taking of high speed movie photographs of the propellant flame. The quenched surfaces of all samples are analysed with a scanning electron microscope. The 24% carboxyl terminated polybutadiene + 76% 25 $\mu$  ammonium perchlorate propellant extinguishes permanently for initial depressurization rates exceeding ca.  $7.5 \times 10^3$  atm/s, when the initial pressure is 45 atm. At the highest depressurization rates ( $>16 \times 10^3$  atm/s), the gaseous flame quenches immediately due to the adiabatic expansion. Lower rates of fall in pressure ( $7 \times 10^3$  to  $16 \times 10^3$  atm/s) allow a second flame to develop after 5 - 7 ms, the relaxation time of the solid phase. This new flame is irregular and partially consumes the AP particles available on the propellant surface, depending on the imposed dP/dt. The driving mechanism is far from one-dimensional. The new flame goes out only at the end of the pressure transient. The restart capability of the propellant is most favorable when the imposed  $(dP/dt)_0$  is considerably above (twice) that required for permanent extinction. The reduction of pressure is never an exponential function of time throughout the transient. Increased AP particle size of the propellant yields qualitatively similar results. Other methods of extinguishing a propellant flame give quenched surfaces with drastically different structural characteristics. The investigation shows that previous one-dimensional and/or linearized theories of propellant burning can not be valid for the phase where the new flame is developed.

---

\* Presented before the 13th International Symposium on Combustion, Salt Lake City, U.S.A., Aug. 23-29, 1970. To be paper for "Combustion Science and Technology"

This research has been sponsored in part by the Air Force Office of Scientific Research through the European Office of Aerospace Research, OAR, United States Air Force under Contract F61052-70-C-0013

<sup>†</sup> Deutsche Forschungs- und Versuchsanstalt für Luft- u. Raumfahrt e.V. (DFVLR)  
Institut für Chemische Raketenantriebe, 3041 Trauen ü. Soltau/Hann., W.GERMANY

## 1. INTRODUCTION

The ever increasing tendency to use solid propulsion units for space missions emphasizes the need for improved economical design to control the instant of terminating the thrust. In some cases it is important also to be able to reignite at a later time. Quenching with a liquid has mechanical complications and the unattractive feature of requiring extra ballast. When a rocket is to be fired only once extinction by depressurization is the most practical. However, for a second firing, devices more ingenious than blowing off the rear end of the rocket must be found. Of immeasurable help to such developmental work is an understanding that predicts as a function of all the important parameters, the depressurization rate required to cause extinction and yet leave the propellant surface in a state allowing easy reignition.

Most of the work done so far for elucidating the rapid depressurization extinguishment process was in the form of parametric extinguished/not-extinguished type studies. In parallel, theoretical efforts were made to predict these findings. The theoretical models were largely based on knowledge gained of the flame structure during steady state burning.

## II. FINDINGS FROM EARLIER WORKS

The main considerations emerging from numerous recent studies (1-13) of the depressurization extinguishment phenomenon are:

The flame of an ammonium perchlorate (AP) composite solid propellant has two exothermic gas phase reaction zones. Both of these are fast compared to the depressurization rate typically required to extinguish an AP propellant. The characteristic time for such an imposed pressure transient is  $10^{-2}$  sec or more; the order of magnitude characteristic times of the thin AP decomposition flame and of the ensuing thicker binder + AP diffusion flame are  $10^{-7}$  sec and  $10^{-5}$  sec, respectively. The solid phase heat-up zone with a time constant of about  $5 \times 10^{-3}$  sec is too slow to be quasi-steady. Because the slow responding solid phase is the boundary to the gaseous flame, neither the burning rate nor the conductive heat feedback from the flame is quasi-steady. Even when we consider the surface layer of the solid thin enough to be quasi-steady, as is probably the case, the heat transfer through that layer can not be quasi-steady.

Previously proposed theories of dynamic burning, for cases where the imposed pressure excursions are large, have been adequately reviewed by Culick (1) and by Merkley et al (2). As pointed out by these authors, most earlier theories (3-7) suffer from either incorrect usage of the quasi-steady approximation, or linearization of a problem that is not linear, or disregard of some fact about the flame structure known to be important, i.e., the influence of AP particle size. Merkle sought to avoid these difficulties and in so doing, modified the granular diffusion flame theory (8) for the nonsteady situation. The extinguished/not-

extinguished predictions as a function of all the important propellant parameters were the most successful of all theories proposed so far. That success is partially due to the fact that the measured pressure transient was taken as input to the theory; the flame behaviour was not coupled to the gasdynamics of the combustion chamber. Some interesting outcomes of the theory are: (a) extinction tends to occur near the end of the transient, (b) the burning rate falls monotonically with reduction pressure, and (c) the rate of chemical reaction becomes more important in controlling the rate of the diffusion flame the faster the rate of fall in pressure. Another interesting approach is that of Zeldovich, Novozhilov et al, recently taken up by Summerfield et al (9). It aims to circumvent the need to know the details of the gaseous flame structure by inferring the conductive heat flux from the gas phase using experimentally determined steady state burning rate measurements. The heat flux into the solid phase, the surface boundary condition, is then known for the transient situation; as long as the gas phase remains quasi-steady it provides the same flux for the same pressure and burning rate. The extinction criteria subsequently developed are based on perturbational considerations. As with previous linearized theories the parameter value predictions tested give the right trends. However, as indicated below, extinction often depends on the entire history of the pressure transient; for instances where the flame quenches near the end of the transient such linearized theories can not hold.

Depressurization extinction data have for the most part been correlated by plotting the initial pressure ( $P_0$ ) against the initial depressurization rate. The relationship was always linear. This relationship can naturally only be accurate when  $P_0$  and  $(dP/dt)_0$  specify the entire pressure curve, i.e., when the chamber  $L^*$  remains constant and when the variation in the (10) rate of gas production by the propellant is not excessive. Thus, Ciepluch and Jensen (11) found that merely increasing the back pressure makes extinction markedly more difficult. Also, Jensen (11) and Merkle (2) noted that combustion chamber geometry ( $L^*$ ) has a profound effect. Nevertheless, until the extinguishment process is understood with sufficient detail, the  $(dP/dt)_0 - (P)_0$  correlation remains helpful.

The many performance type extinction tests (Refs. 2-11), particularly those of Jensen and of Merkle, show that an AP composite propellant is harder to extinguish when: (a) the AP content is increased, (b) the AP particle size is reduced, (c) the percentage of AL powder is increased, (d) Al needles are introduced, and (e) copper chromite catalyst is added. The binder type has comparatively small effect on the extinguishment behaviour. The causes of these small binder effects have not been identified.

Very few detailed measurements of the flame behaviour during the course of a rapid pressure reduction have been made. There is still ambiguity as to whether the burning rate behaviour during the pressure fall is monotonic, how the flame structure alters itself and what its effect might be, and whether extinction can be so accomplished to make a restart easier. Shelton's (12) microwave measurements can not be highly accurate

but they do suggest that several swings in the burning rate are possible. Baer, Schultz and Ryan (13) made infrared spectroscopic measurements of the  $\text{CO}_2$  and  $\text{H}_2\text{O}$  bands and concluded that initially, the fuel/oxidizer mixture ratio of the gas phase flame drops, but after 10-20  $\mu\text{s}$ , it increases again and reaches a maximum. The earliest total luminous intensity measurements made by Ciepluch (10) show also that the gas phase flame can redevelop once. Our work is directed at these questions. We do this by taking intensity measurements of several spectral lines together with high speed movie photographs and then we examine the quenched propellant surface with a scanning electron microscope.

### III. APPARATUS AND PROCEDURES

The experimental set-up is shown schematically in Fig. 1. The pressure vessel, capable of operating at 200 atm pressure, consists of two quartz side-windows, a nitrogen inlet port, two small side-vent nozzles, and a large pressure release nozzle that is kept closed by the double diaphragm device until when the rapid depressurization is to occur. In an actual test the nitrogen is allowed to flow past the propellant strand until just before ( $\sim 50$  ms) the two burst discs blocking the main nozzle are broken by releasing the preset pressure in the cavity between these discs. The moment of opening of the main nozzle is controlled to occur soon after the solid propellant comes into the field of view of the camera and of the spectrograph. The depressurization rate is varied from test to test by changing the diameter of this main nozzle.

The propellant sample is 1,5 cm thick and the faces viewed by both the camera and the spectrograph are 2,5 cm x 3,5 cm. The camera and the spectrograph respectively see a zone of length 1,5 cm and 0,5 cm in the propellant flame. A planar regressing surface is achieved by covering the ignition surface with a fast flashing material that is in turn ignited by an electrically heated nichrome wire. The side surfaces of the sample are inhibited by leaching with water and then converging with a film of silicone oil.

The entire electronic system for all measurement signals has been layed out for a frequency response of 20 kHz. The piezoelectric pressure transducer is water cooled and has its diaphragm mounted almost flush with the inside wall of the combustion chamber. The spectrograph, Hilger and Watts type E 498, has been modified so that the intensities of the OH, NH, CN, and Na lines can be measured individually with IP28 photomultipliers. The maximum bandwidth of each of these lines is 80 Å. For comparative purposes, the intensity of a spectral window of similar bandwidth in the carbon continuum range at 4880 Å is also measured. All these DC signals are amplified and fed into a high frequency response tape recorder for later replay into a galvanometer recorder. Replay is at 100 - 200x expansion of the time scale.

All extinguished samples were photographed at high magnification (up to 2000 x) using a scanning electron microscope (SEM), Cambridge Instruments Co. (MK 2A). To obtain pictures with the highest quality, these samples were first prepared by vaporising a thin composite layer of graphite-gold-graphite into the surface. On occasion, stereoscopic photos were also made to help in the interpretation of difficult cases. Wherever, possible, the exposed AP particles were measured to determine the AP coverage area and the AP particle size distribution. At least 1000 particles were measured to determine each distribution curve.

#### IV. EXPERIMENTAL RESULTS

The results of this paper are for a 76% AP propellant with 24% carboxyl terminated polybutadiene binder (PBCT). Two propellants were chosen, one with 25  $\mu$  mean AP particle size and the other with 200  $\mu$  mean AP size, both determined by sieve analysis. This size distribution of the former is relatively broad (about 10% by weight of 100  $\mu$  AP particles exist in the distribution). Both propellants were supplied by Bayern Chemie GmbH of W. Germany.

In all the tests of this study, the pressure just before the onset of the depressurization was adjusted to  $44,5 \pm 2,5$  atm. These slight variations in initial pressure ( $P_0$ ) were removed in the data reduction by normalizing all pressures with respect to this  $P_0$ . The exhaust pressure is constant at atmospheric pressure.

The spectroscopic measurements of this study are for a zone of dimensions 0,5 cm x 0,02 cm in the gaseous flame. The height of this measurement zone is 0,1 cm to 0,3 cm above the propellant surface when the depressurization starts.

The tests conducted in the series for the propellant with fine ground AP are summarized in Table I. The connection between the many different measurements of each test is best followed when the descriptive sections below are kept in reference to this table. All tests are identified by their initial depressurization rates,  $(dP/dt)_0$ .

##### (a) Measurements from a Single Depressurization Test

Fig. 2(a) gives the measurement traces obtained in a test with the highest imposed depressurization rate ( $25 \times 10^3$  atm/s) of the series for the 25  $\mu$  AP propellant. Included is a movie sequence of the flame behaviour. This measurement trace shows that the Na intensity, an indication of the temperature of the gases, falls to zero within 1 ms. The ratio of instantaneous pressure to initial pressure ( $P/P_0$ ) at this time ( $I_{Na} = 0$ ), is 0,66. A series of rarefaction and compression waves reflected back and forth in the combustion chamber is recognizable in the initial parts

TABLE 1 SUMMARY OF DEPRESSURIZATION TESTS FOR  
24 % PBCT + 76 % 25  $\mu$  AP PROPELLANT

(dP/dt) <sub>o</sub> (atm/s)	P <sub>o</sub> (atm)	(P/P <sub>o</sub> ) at I <sub>Na</sub> =0	REDEVELOPED FLAME?		PERMANENT EXTINCTION?	QUENCHED SAMPLE	
			START (ms)	END (ms)		STRUCTURE	AREA FRACTION COVERED BY AI
25x10 <sup>3</sup>	47	0,66	NO	NO	YES	EXPOSED AP	0,70
25x10 <sup>3</sup>	47	0,60	NO	NO	YES	EXPOSED AP	NOT MEASURED
16x10 <sup>3</sup>	45	0,75	8(?)	13(?)	YES	CENTER: EXPOSED AP EDGES: LESS AP	0,43 0,25
13x10 <sup>3</sup>	42	0,78	5	30	YES	CENTER: LESS AP EDGES: MAINLY HOLES	0,45 0
13x10 <sup>3</sup>	45	0,74	5,6	33	YES	CENTER: LESS AP EDGES: ONLY HOLES	0,48 0
8,2x10 <sup>3</sup>	46	0,80	5	39	YES	ONLY HOLES	0
6,7x10 <sup>3</sup>	45	0,77	4,5	62	NO	--	--
2,6x10 <sup>3</sup>	42	--	FLAME STAYS		NO	--	--

of both the pressure and Na intensity traces. The jumps in the P and I<sub>Na</sub> traces are of opposite phase because the flame zone and pressure transducer are situated on opposite sides of the chamber; the approximately 0,2 ms period corresponds to the theoretical value for a chamber of 10 cm length.

The intensity of the carbon continuum lags 0,8 ms behind that of the Na line. In a general sense, the CN intensity follows that of the Na; the temperature sensitivity of this radicle emission is, expectedly, very strong. The NH and OH intensity measurements have no fundamental meaning for the present test series because these lines for this underoxidized PBCT propellant are too weak to be measured (confirmed by independently taken spectrographs). The slight intensity shown by the NH trace is probably due to carbon continuum whose radiation reaches the 336 nm wavelength range (also indicated by the spectrographs).

#### (b) Reproducibility of Results

Fig. 2(b) shows the measurement trace and movie sequence obtained for the same conditions as that of Fig. 2(a). The measured (dP/dt)<sub>o</sub> is now 23 x 10<sup>3</sup> atm/s. Eventhough the (dP/dt)<sub>o</sub> can be only determined with 10% accuracy, the normalized pressure traces of both tests are identical (see Fig. 5).



The reproducibility overall for the above very fast depressurization is very good. Figs. 3 and 5 show the reproducibility for a slower depressurization rate ( $13 \times 10^3$  atm/s) to be less good. As is to be shown later, this is due to the development of a new flame that is irregular for intermediate values of  $(dP/dt)_0$ .

The reproducibility of the surface structure of quenched samples is to be discussed in part (d) of this section.

### (c) Effect of Depressurization Rate

The  $(dP/dt)_0$  was varied over an order of magnitude from  $2 \times 10^3$  atm/s to  $26 \times 10^3$  atm/s. Figs. 2 and 3 show some of the traces obtained. The results are summarized by Table I and Fig. 5.

For  $(dP/dt)_0 > 16 \times 10^3$  atm/s, the flame intensity falls to zero within the first millisecond. The same is true for still lower values of  $(dP/dt)_0$ . However, then, a second flame develops after about 5 ms. This new flame does not go out until the pressure has just about equalized with the back pressure; the difference between the extinction pressure and the exhaust pressure can not be detected with accuracy. For  $(dP/dt)_0 < 7.5 \times 10^3$  atm/s, the newly developed flame does not go out at all; the propellant burns up completely. In these cases of low  $(dP/dt)_0$ , the flame intensity does not quite reach zero in the period 1 ms to 5 ms. However, it is significantly reduced. Except for these two slow cases, the ratio  $(P/P_0)$  at which the flame intensity becomes zero, falls between 0.60 and 0.80.

The  $\log [(P-P_f)/(P_0-P_f)]$  vs. time plots of Fig. 5 show that in no case is pressure variation an exponential function of time. Only in the cases where no new flame develops can a straight line be drawn to a portion of the curve\*. Otherwise, there is a strong tendency for the pressure to oscillate as it falls.

### (d) Surface Structure of Depressurization Extinguished Samples

Figs. 6 to 9 summarize our observations of the structure of the quenched propellant surface as a function of the initial depressurization rate. In our description below we concentrate on the characteristics of AP particles whose order of magnitude is  $1 - 20 \mu$ . The very few large particles noticeable are the exception and are therefore not important from an overall combustion mechanistic standpoint. Moreover, their appearance is generally the same regardless of the depressurization rate.

---

\* The concave upward shape of the logarithmic pressure-time curves during the first few milliseconds is not likely to be due to the influence of some small residual  $N_2$  flow (that sometimes is evident from the fact that the flame temperature of the redeveloped flame goes a little above the steady state value); the shutting time of the  $N_2$  supply valve is not reproducible to within the millisecond, yet the reproducibility of the pressure-time traces is reproducible to much greater accuracy. Tests are planned that avoid the  $N_2$ -flow completely. They will settle any remaining doubts.

Fig. 6 gives several magnifications of the geometric structure of a sample extinguished with an intermediate  $(dP/dt)_0 = 13 \times 10^3$  atm/s, i.e., for the case where a secondary irregular flame was developed (see Figs. 3 - 5). Two vastly different structured surface-types exist depending on the location on the sample surface. The region in the middle of the sample has clearly defined AP particles sticking out above the binder surface. However, around the edges of the sample only the exceptional exposed AP particle can be discerned; in the main, there are holes out of which the AP particles have apparently been burned. The outer region of the burned surface is situated below the central portion, as if a flame had preferentially consumed it. The difference in height of the step at the transition zone (measured with an optical microscope) is  $75 \mu \pm 25 \mu$ . In the case of this test, the redeveloped flame burned for 25 ms. If we assume that this redeveloped flame caused the step in the quenched surface we note that the average burning rate must then have been about 0,3 cm/s. This value has the right order of magnitude.

Fig. 7 shows the effect of varying  $(dP/dt)_0$ . The middle set of pictures is of the step transition zone for the intermediate  $(dP/dt)_0$  case described above. The step is well defined and the dramatic change in the character of the surface is also obvious. The other pictures are for the extremes of high and low  $(dP/dt)_0$ , for which quenching was still possible. In both these very high and low  $(dP/dt)_0$  cases, the microscopic structure of the surface remained the same across the entire surface, including the regions near the edges of the sample: at the high  $(dP/dt)_0 = 25 \times 10^3$  atm/s, partially exposed AP particles are seen; at the low  $(dP/dt)_0 = 8,2 \times 10^3$  atm/s there are only holes. The region at the edges of the intermediate  $(dP/dt)_0 = 13 \times 10^3$  atm/s sample is like that of the low  $(dP/dt)_0$  case and the central region is like that of the high  $(dP/dt)_0$  case, only now a larger fraction of the burning surface area occupied by the exposed oxidizer particles.

Fig. 8 is presented to show the reproducibility of the quenched surface structure at the same intermediate  $(dP/dt)_0$ . They also to show the alterations in structure caused by changing  $(dP/dt)_0$  slightly. Fig. 8(a) is a new test for  $(dP/dt)_0 = 13 \times 10^3$  atm/s, the same condition as that of Figs. 6(a) and 7(b). The results are qualitatively the same. Comparison of Figs. 8(a) and 8(b) show the alterations caused by an increased  $(dP/dt)_0$  of  $16 \times 10^3$  atm/s: the central portion looks that as that for the  $(dP/dt)_0 = 13 \times 10^3$  atm/s case of Fig. 8(a); the region around the edges has some AP particles exposed (the  $13 \times 10^3$  case does not). The redevelopment of a flame can only barely be detected (see Fig. 5(a)). In the case where  $(dP/dt)_0 = 16 \times 10^3$  atm/s. It is of low intensity and short-lived (perhaps 5 ms, as opposed to 25 ms for the previous cases). Thus it is clear that the oxidizer particles in the regions near the sample edges could only be partially consumed. The conclusion is better proved by the AP particle size distribution measurements of the next section.

It is important to note that all the high magnification SEM pictures of Figs. 6 to 9 show the binder surface to be smooth. The impression is that

it was molten. However, this molten layer is no thicker than a few microns. Only in isolated instances could flakes of binder be identified. Stereoscopic SEM pictures showed that these few exceptional flakes reach far out above the propellant surface.

#### (e) Size Distribution of AP Particles on Depressurization Quenched Samples

Wherever exposed AP particles could be identified, the size distribution was measured and then plotted in Fig. 9, as cumulative exposed AP surface area versus AP particle diameter\*. Because most of the surfaces of Figs. 6-8 were devoid of AP particles, only those identified as samples B, C, E, and F could be measured i.e., those not significantly, or not at all disturbed by the development of a secondary flame.

Fig. 9 (see also Table I for summary) shows that the propellant sample extinguished at the highest depressurization rate imposed ( $25 \times 10^3$  atm/s) has the largest fraction of its area covered by exposed AP particles. When the depressurization rate is lowered to a value just low enough that a new flame barely develops, i.e.,  $(dP/dt)_0 = 16 \times 10^3$  atm/s, the AP particles on the surface are apparently partially consumed. The consumption around the edges is significantly more than in the center of the sample. Further lowering of  $(dP/dt)_0$  to  $13 \times 10^3$  atm/s leaves the center of the sample with about the same coverage as for the case  $(dP/dt)_0 = 16 \times 10^3$  atm/s. However, around the edges all AP particles have been burned out of the surface and only holes remain. Finally, at the lowest  $(dP/dt)_0$  where permanent extinction is possible ( $8.2 \times 10^3$  atm/s), even the central regions of the sample are devoid of AP particles.

The above measurements of AP surface coverage, in conjunction with the previous SEM picture series, clearly shows that when the redeveloped flame occurs, it preferentially consumes the AP and does so from the outer regions of the sample inwards. It implies that the oxidizer/fuel mixture ratio of the flame changes and is higher than during steady state burning. It is interesting that the mean AP particle size remains the same despite these variations.

---

\*

$$\left\{ \sum_{d=c}^{d=d} (n_d d^2) \right\} / \left\{ \sum_{d=c}^{d=m} (n_d d^2) \right\} \quad \text{vs.} \quad (\log d)$$

where  $n_d$  is the number of particles of diameter  $d$ . This method of representation is a relative indicator for the AP to binder gasification area and hence the oxidizer/fuel mixture ratio of the gaseous flame. Distortions from the real oxidizer/fuel ratio are of course likely because of the obvious 3-dimensional character of the quenched propellant surface on a microscopic scale.

There was some difficulty measuring the particles of the highest ( $dP/dt$ ) case because they tended to merge with the surrounding molten binder. This may be reason why the measured AP coverage fraction seems a little high in this case. The situation is being re-analysed.

(f) Effect of Original AP Particle Size in Propellant

The previous depressurization extinguishment series has been repeated for the same propellant type except that now the average AP particle size is far larger, 200  $\mu$ . The results are generally speaking qualitatively the same. The initial depressurization rate required for extinction is about the same as that for the previous small particle size propellant. For the larger particle size propellant, a flame also redevelops at the lower imposed initial depressurization rates but it is less intense and only persists half as long as it does for the fine AP propellant under the same conditions. Two SEM picture series of the highest and the lowest imposed depressurization rates (see Fig. 10) show that the parts of the extinguished surface area between the large exposed AP particles have the same general characteristics as those previously found with the small particle size propellant. The large particles regress flush with the surrounding molten binder. They show no significant alteration in appearance when the depressurization rate is varied over the range investigated. More detailed analysis is necessary.

(g) Effect of Quenching Method on Propellant Surface Structure

A wide variety of methods of extinguishing the propellant flame were imposed: (1) blowing nitrogen at  $-190^{\circ}\text{C}$ ; (2) blowing nitrogen at  $+20^{\circ}\text{C}$ ; (3) blowing preheated nitrogen of unknown temperature; (4) allowing the propellant to burn out on a metal plate; (5) reducing ambient pressure to below the natural low pressure extinction limit of the propellant. The surface structures obtained by these methods for both the 25  $\mu$  and the 200  $\mu$  AP propellant types are shown in Figs. 11 to 13.

Inspection of the set of pictures in these figures allow some interesting observations. None of the five quenching methods tried give a surface structure that is similar to those observed when quenching by rapid depressurization. Of these five methods, blowing with  $\text{N}_2$  at temperatures below  $20^{\circ}\text{C}$  appears to quench the flame most effectively; the quenched surface is smooth, though the ridges could have been formed by the nitrogen forcing the molten binder to flow for a short time. The 3 other quenching methods allow post-reactions to continue long enough that deep holes are bored into the quenching surface. Again, AP is preferentially consumed during the quenching process. The depth of the porous layer formed seems smallest when preheated nitrogen is used and is the largest when the propellant is extinguished by reduction of pressure below the low pressure limit.

## V. DISCUSSION AND CONCLUSIONS

The experimental observations of the previous section all fall into a consistent picture:

(a) It is shown that only for the most rapidly imposed initial depressurization rates ( $> 16 \times 10^3$  atm/s), does the gaseous flame quench within the earliest part of the pressure transient. This usually occurs within the first few milliseconds but in any case, when the pressure has reached the value  $(P/P_0) = 0,70 \pm 0,10$ . Though, as evidenced by the strong influence on the flame intensities of the impinging rarefaction and compression waves, adiabatic expansion is the main cause for the reduction in flame intensity, it is not the full explanation; the fall in temperature from  $1950^\circ$  K (the adiabatic flame temperature of the propellant (2,13)) to about  $1600^\circ$  K (the temperature where a flame generally loses its luminous intensity) due to the reduction in  $(P/P_0)$  from unity to  $0,70 \pm 0,10$ , can only be explained on the basis of adiabatic expansion when an unrealistically small of  $\gamma$  (the specific heat ratio) is assumed. Adiabatic expansion must cause the temperature to drop sufficiently to quench the chemical reactions prevailing and then the temperature drops even faster. This contention is not surprising. It is supported by the observation that the intensity of the CN radicle always drops far faster than that of the Na line. The intensity of the carbon continuum usually lags behind by  $0,7 - 1,0$  ms. The cause is likely to be in the thermal inertia of glowing carbon particles.

(b) When the initial depressurization rate is  $16 \times 10^3$  atm/s and lower, a new flame always develops after 5 to 7 ms, approximately the thermal lag time of the solid phase. The observation is well explained by the fact that the gaseous flame, being quasi-steady, quenches in accordance with the instantaneous pressure. However, the solid phase needs a certain time to adjust to the new conditions to supply the necessary combustibles for a new flame. The gases must still be hot enough to allow ignition of these combustibles if a new flame is to form, i.e., the  $(dP/dt)_0$  may not be above  $16 \times 10^3$  atm/s in the case of the propellant studied here.

(c) In case where the new flame is formed, it is irregular and prefers to sit nearer the edges of the propellant sample\*; only for  $(dP/dt)_0 < 10 \times 10^3$  atm/s does it spread over the entire surface area of the sample. The SEM investigations show that the redeveloped flame preferentially consumes AP from the surface of the propellant. The implication is that the oxidizer/fuel ratio of the new flame increases. Ryan et al's infrared spectroscopic measurements (13) of the  $H_2O$  and  $CO_2$  bands indicate that the oxidizer/fuel ratio increases for the first 10 to 20 ms and then decreases afterwards. This reduction of the O/F mixture ratio is perhaps the cause, in our results, for the lowering of flame intensities consistently after 10 - 15 ms.

---

\* This preference is unexpected and curious. The cause for this behaviour must still be found.

(d) The lack of AP particles in samples quenched with lower depressurization rates indicates poorer restart capability. In the case of an actual rocket motor application, the medium depressurization is preferable for extinction for two reasons: to extinguish safely and yet leave a fuel covered surface which can not easily be reignited by some hot parts of the motor case. Experiments designed to determine the energy required for a reignition are needed to see whether the consideration is of practical importance.

(e) When the secondary flame develops it only extinguishes near the very end of the pressure transient when the pressure is hardly discernable from the back pressure. Thus, the imposed  $(dP/dt)_0$  alone can never be used to predict all the extinction characteristics of a propellant if the behaviour of the redeveloped flame and its concomitant transient mixture ratio changes are not accounted for.

(f) The variation of pressure is an exponential function of time only after the first 4 to 5 ms of the process. During the earliest portion of the transient the  $\log(P)$  vs.  $t$  curve bends concave upwards. This is best explained by the fact that the mass flow through the choked nozzle is inversely dependent on the gas temperature; this temperature falls fast during the first few milliseconds.

(g) The propellant with 20  $\mu$  mean AP particle diameter does not extinguish for  $(dP/dt)_0 < 7,5 \times 10^3$  atm/s. This limit is similar for the large particle size propellant. The approximately obtained critical extinguishing  $(dP/dt)_0$  agrees well with measurements of the same propellant type obtained by other investigators (2,13).

(h) The method of extinguishing influences strongly the overall characteristics of the quenched surface. Methods other than depressurization at very high rates can not be used to infer the structure of the surface during steady state burning. The other methods often relied upon cause distortion of the surface or allow post-reactions that lead to porosity of the surface; AP is burned out of the surface during the quench.

The present study has brought to the fore many new detailed aspects of the behaviour of a solid propellant flame during the imposing of a rapid reduction in pressure. Systematic investigation of the dependence of these phenomena on the many various important propellant composition variables and combustion chamber operating parameters is planned for the future.

## REFERENCES

- 1 Culick, F.E.C. "A Review of Calculations for Unsteady Burning of a Solid Propellant", AIAA J., Vol.6, No.12, December 1968 pp. 2241-2255
- 2 Merkle, C.L., Turk, S.L. and Summerfield, M. "Extinguishment of Solid Propellants by Depressurization: Effects of Propellant Parameters", AIAA Paper No. 69-176, January 1969, also, AMS Report No. 880, July 1969, Princeton University, Princeton, N.J.
- 3 Denison, M.R. and Baum, E. "A Simplified Model of Unstable Burning in Solid Propellants", ARS J., Vol.31, No.8, August 1961 pp 1112-1122
- 4 von Elbe, G. and McHale, E.T. "Extinguishment of Solid Propellants by Rapid Depressurization" AIAA J.
- 5 Brown, R.S., Muzzy, R.J. and Steinle, M.E. "Surface Reaction Effects on the Acoustic Response of Composite Solid Propellants" AIAA J., Vol.6,, 1968, p. 479
- 6 Horton, M.D., Bruno, P.S. and Graesser, E.C. "Depressurization Induced Extinction of Burning Solid Propellant" AIAA J., Vol.6, 1968, p. 292; also, Coates, R.L. and Horton, M.D. "Predicted Effects of Motor Parameters on Solid Propellant Extinguishment", AIAA Paper No. 70-664, June 1970
- 7 Marxman, G.A. and Wooldridge, C.E. "Effect of Surface Reactions on the Solid Propellant Response Function" AIAA J., Vol.6, 1968, p. 471; also "A Comparison between Theoretical and Experimental Extinction Behaviour of Composite Solid Propellants", AIAA Paper No. 70-666, June 1970
- 8 Summerfield, M., Sutherland, G.S., Webb, M.J., Taback, H.J. and Hall, K.P. "Burning Mechanism of Ammonium Perchlorate Propellants" Solid Propellant Rocket Research, Progress in Astronautics and Rocketry Series, Vol.1, Academic Press, New York, 1960, pp. 141-182; also, Steinz, J.A., Stang, P.L. and Summerfield, M., AIAA Preprint No. 68-658, June 1968

- 9 Summerfield M., Caveny, L.H., Battista, R.A., Kubota, N., Gostintsev, Y.A. and Isoda, H. "Theory of Dynamic Extinguishment of Solid Propellants with Special Reference to Nonsteady Heat Feedback Law", AIAA Paper No. 70-667, June 1970
- 10 Ciepluch, C. "Effect of Rapid Pressure Decay on Solid Propellant Combustion", ARS J., 31, No. 11, November 1961, pp. 1584-1585
- 11 Jensen, G.E. and Brown, R.S. "An Experimental Investigation of Rapid Depressurization Extinguishment" AIAA Paper No. 70-665, June 1970; also, NASA CR-66488, Final Report, Contract No. NAS 1-7815, United Technology Corp., March 1969
- 12 Shelton, S., presented at 3rd ICRPG/AIAA Joint Propulsion Conference, Atlantic City, N.J., June 1968, cited by Culick F.E.C. "Remarks on Extinguishment and the Response Function for a Burning Solid Propellant", AIAA J., Vol.7, No.7, June 1969 pp. 1403-1404
- 13 Baer, A.D., Schultz, E.M. and Ryan, N.W. "Spectra and Temperature of Propellant Flames during Depressurization", AIAA Paper No. 70-663, June 1970.



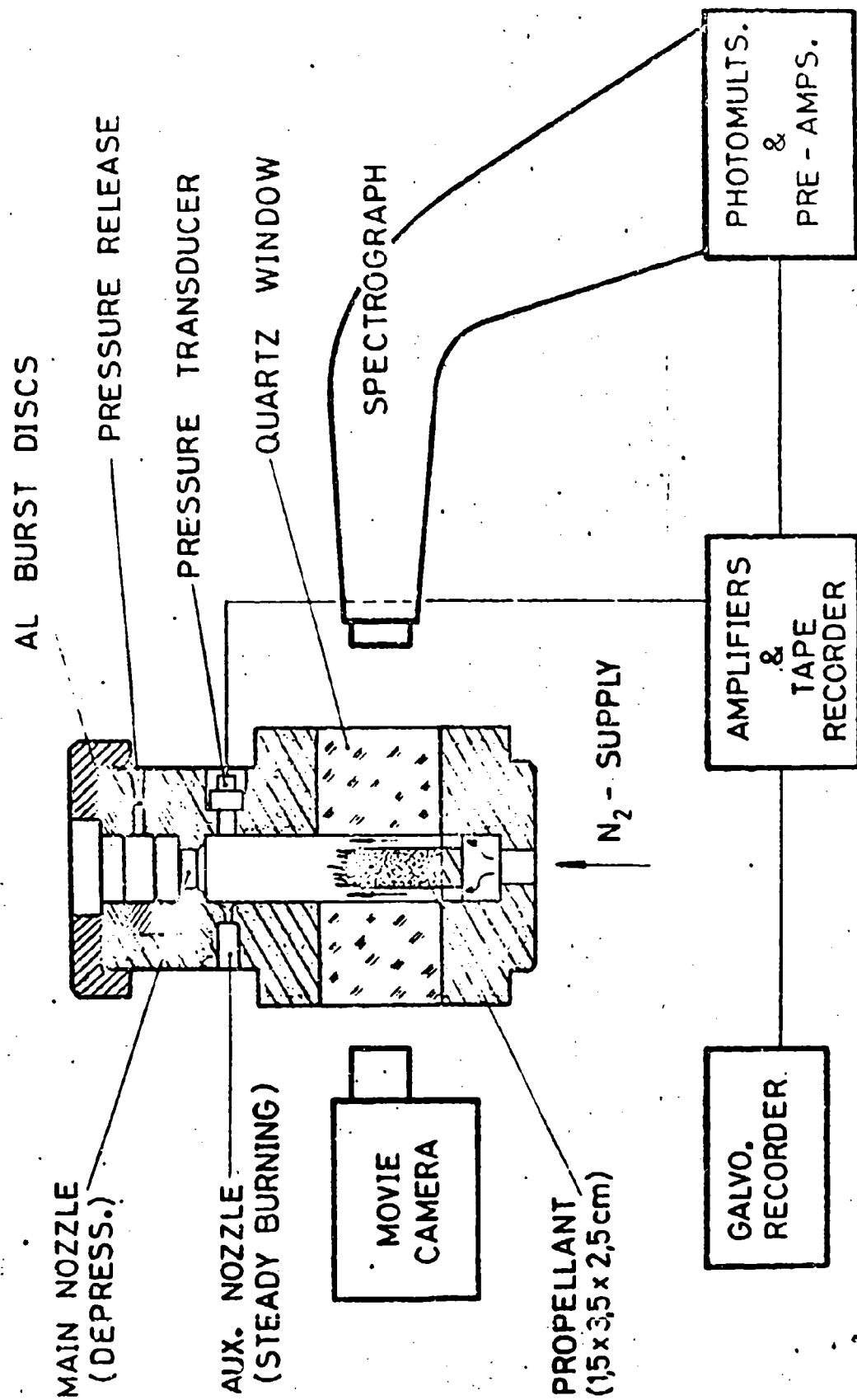
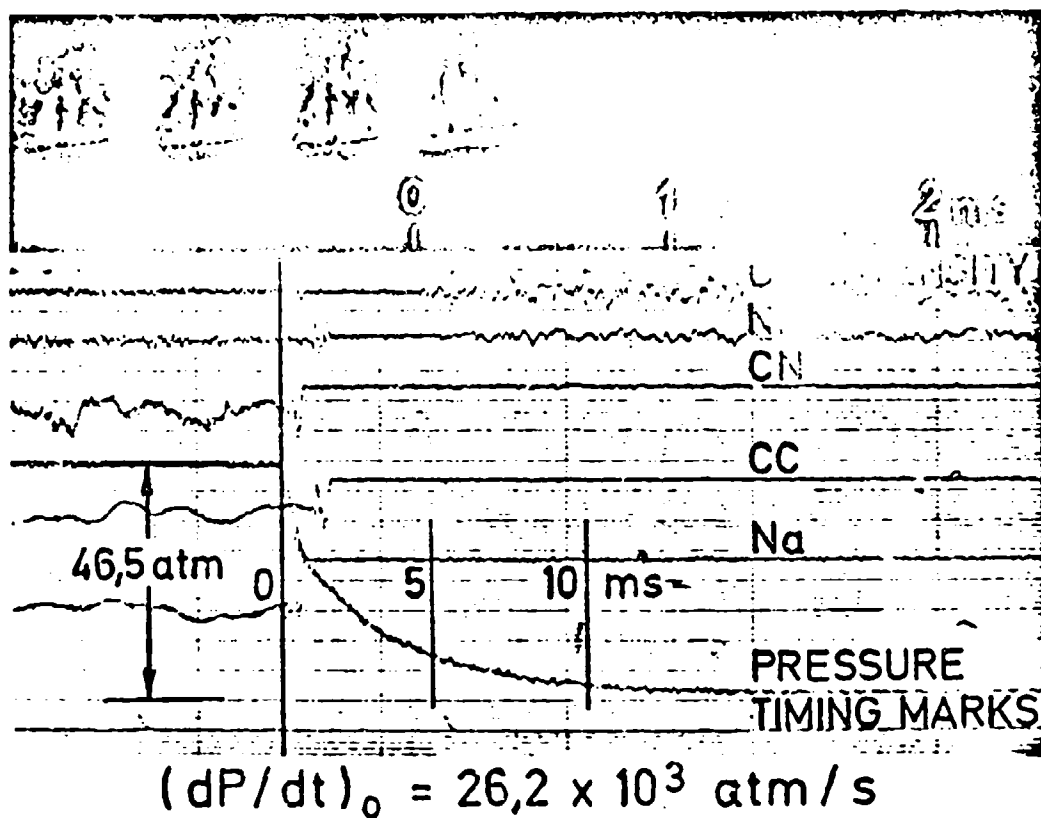
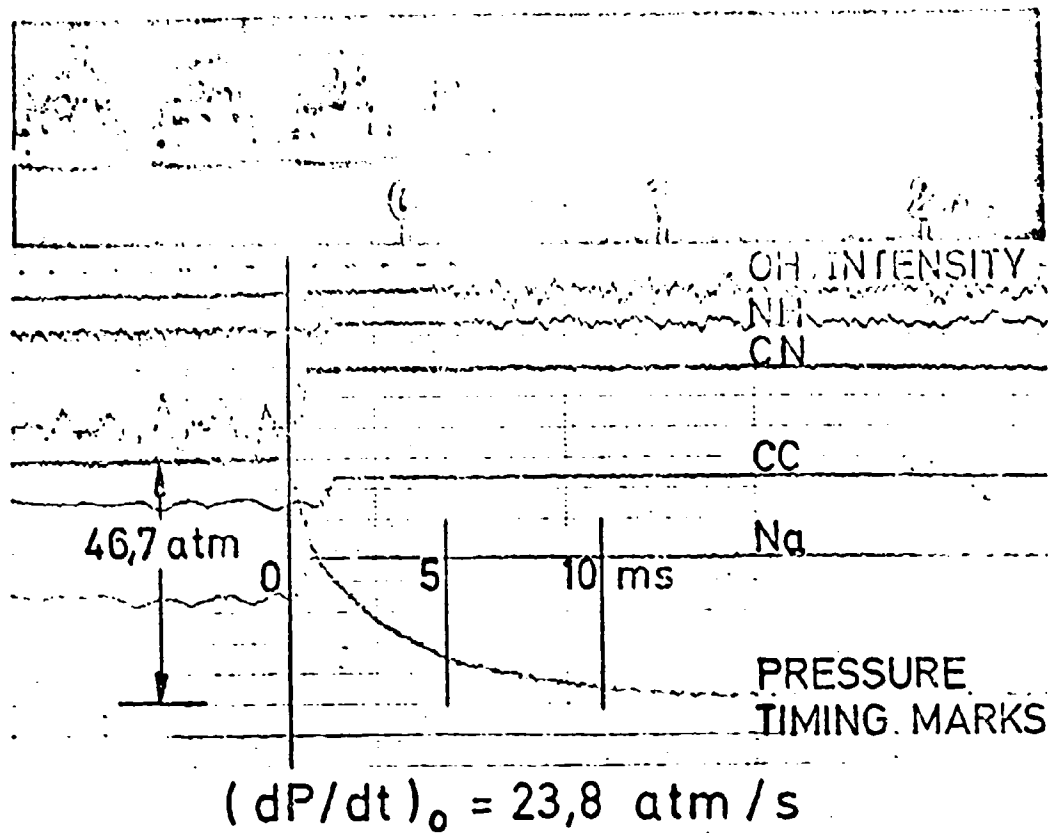
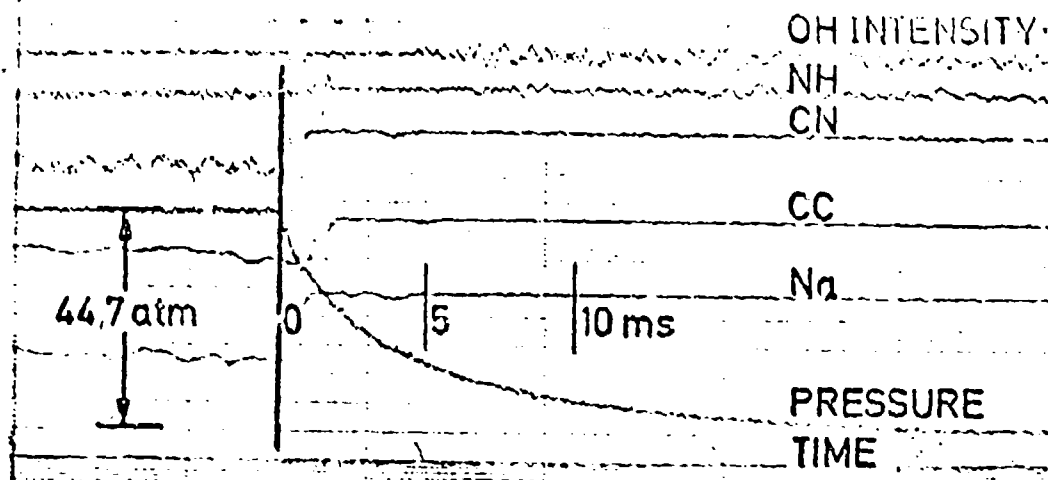


FIG1 DEPRESSURIZATION EXTINCTION EQUIPMENT

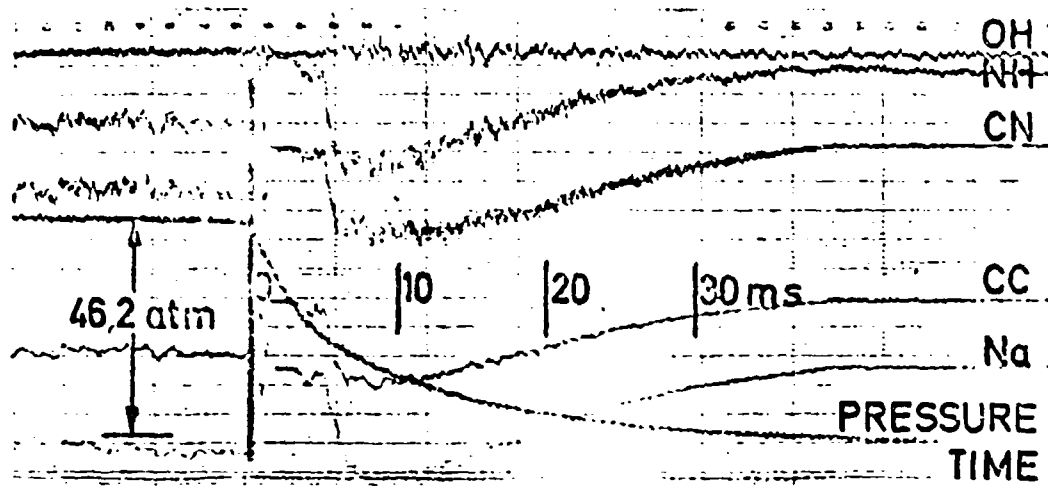


TWO TESTS FOR SAME  $(dP/dt)_0$

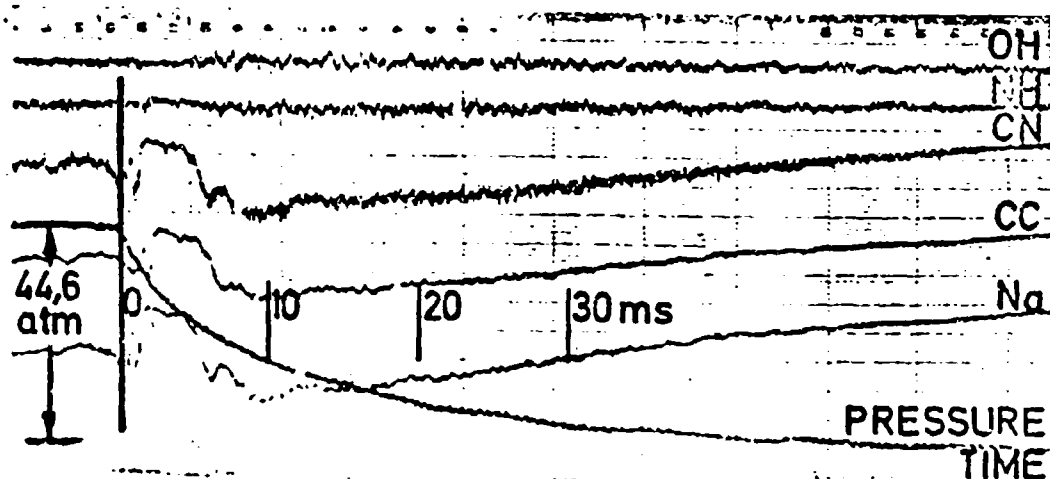
Fig 2



(a)  $(dP/dt)_0 = 16,3 \times 10^3 \text{ atm/s}$

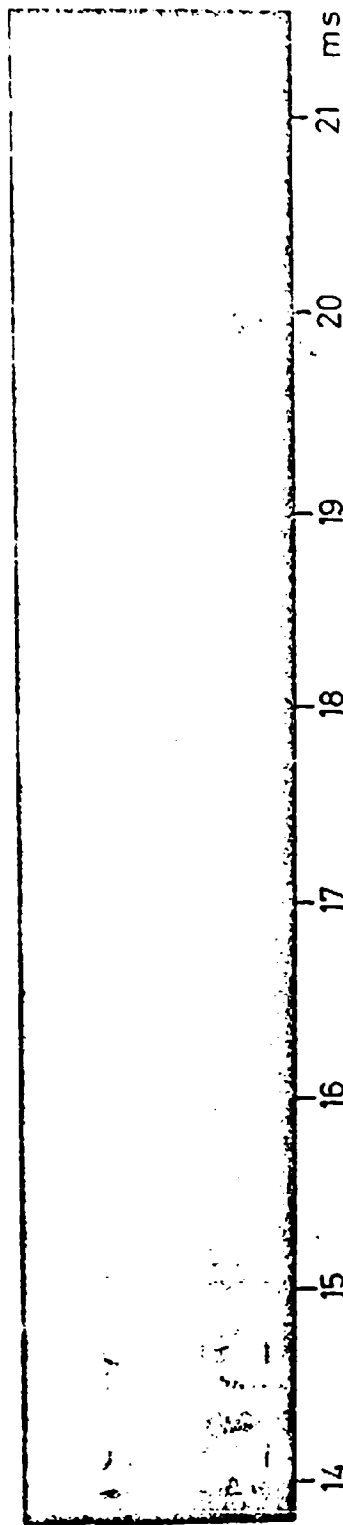
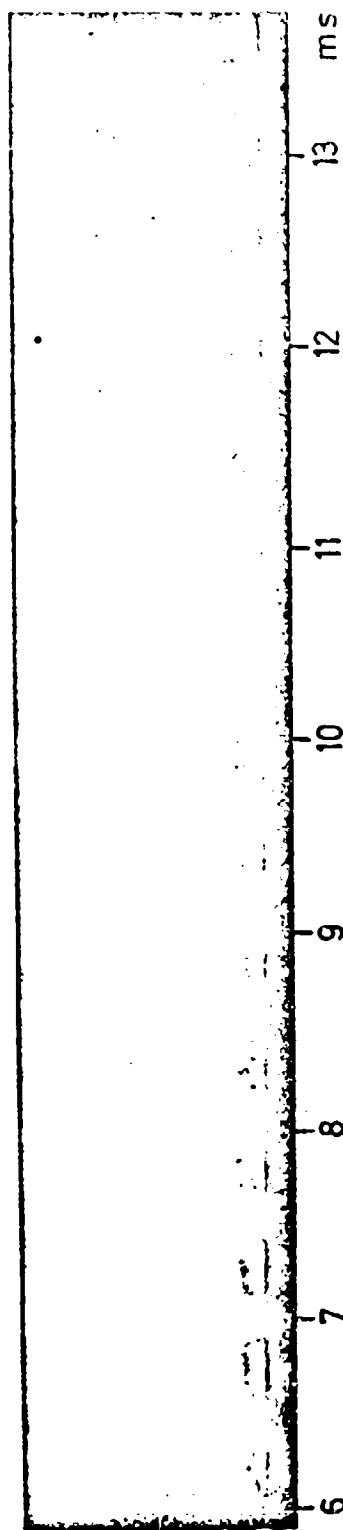
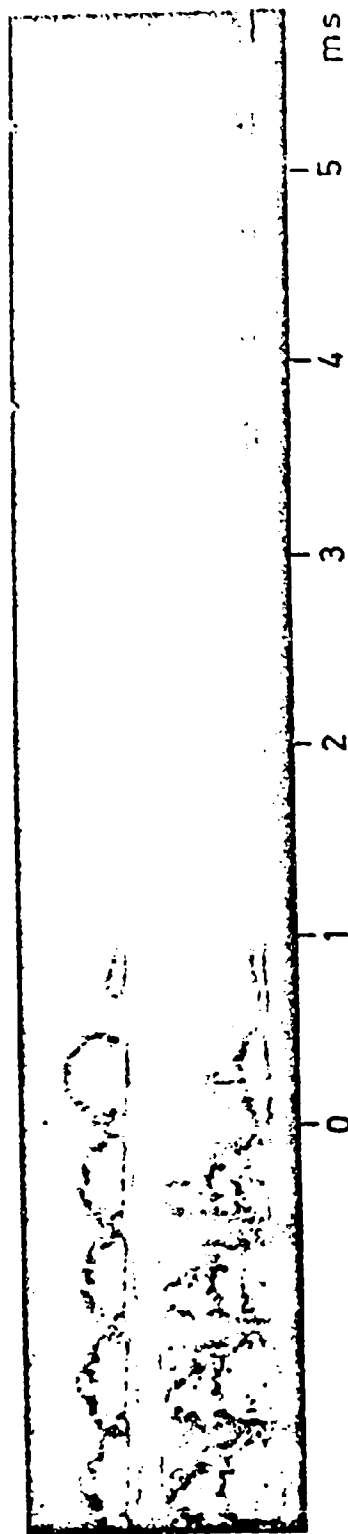


(b)  $(dP/dt)_0 = 3,2 \times 10^3 \text{ atm/s}$



(c)  $(dP/dt)_0 = 6,7 \times 10^3 \text{ atm/s}$

EFFECT OF  $(dP/dt)_0$  ON FLAME BEHAVIOR



MOVIES OF FLAME FOR  $(dP/dt)_0 \approx 13 \times 10^3 \text{ atm/s}$   
( TWO SEPERATE TESTS )

Fig 4

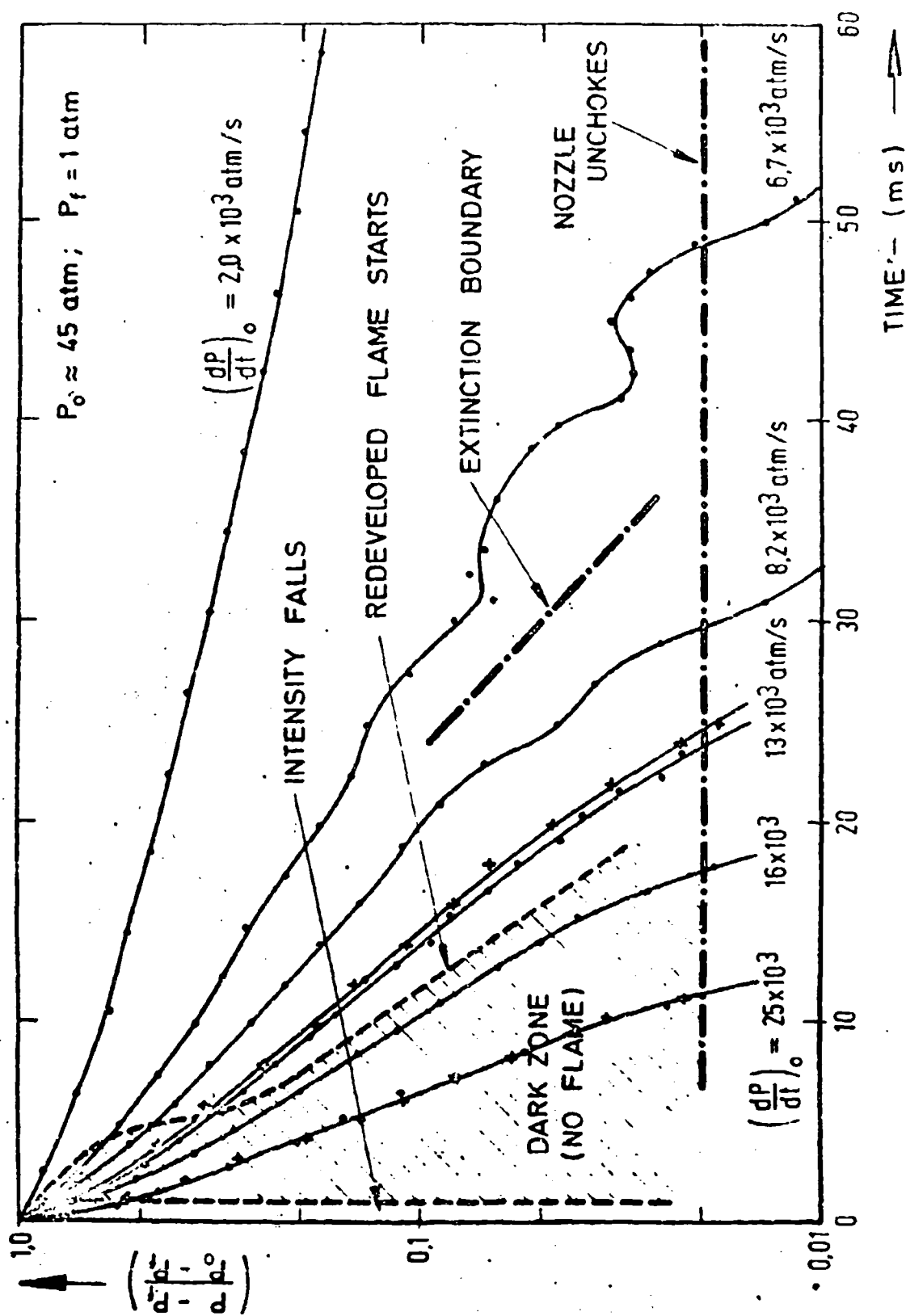
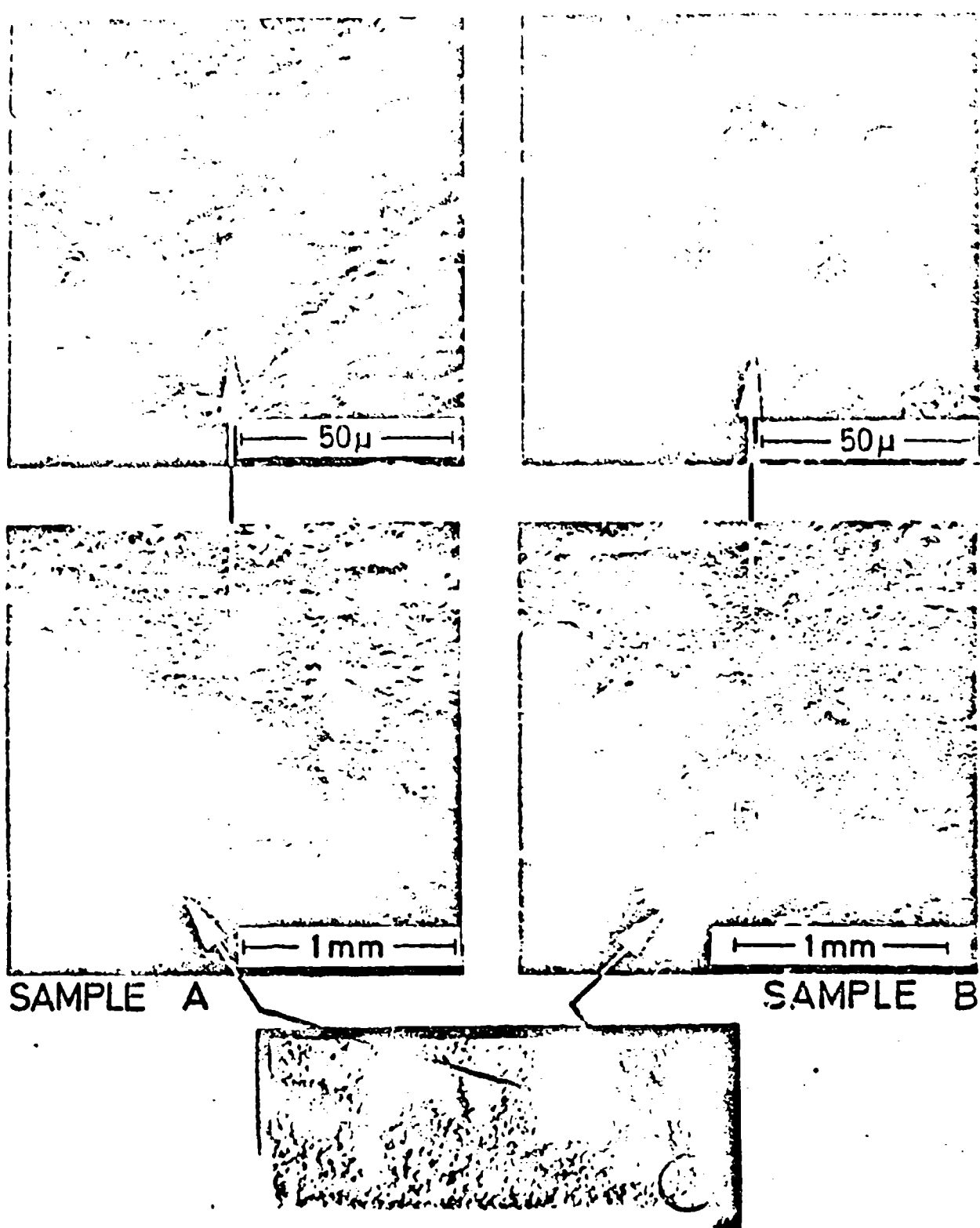


FIG 5  
 MEASURED PRESSURE AND FLAME BEHAVIOR DURING  
 DEPRESSURIZATIONS FOR 24% PBCT + 76% AP ( 25  $\mu$  )



SURFACE STRUCTURE FOR  $(dP/dt)_0$   
 $= 13 \times 10^3 \text{ atm/s}$   
 ( 24 % PBCT + 76 %  $25\mu$  AP )

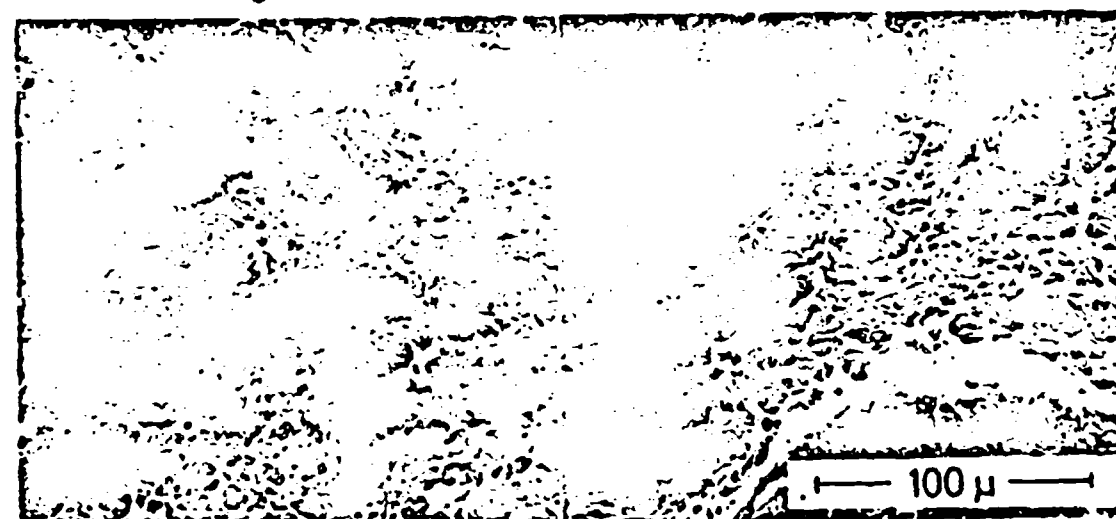
Fig. 5



a)  $(dP/dt)_0 = 25 \times 10^3 \text{ atm/s}$  ( SAMPLE C )

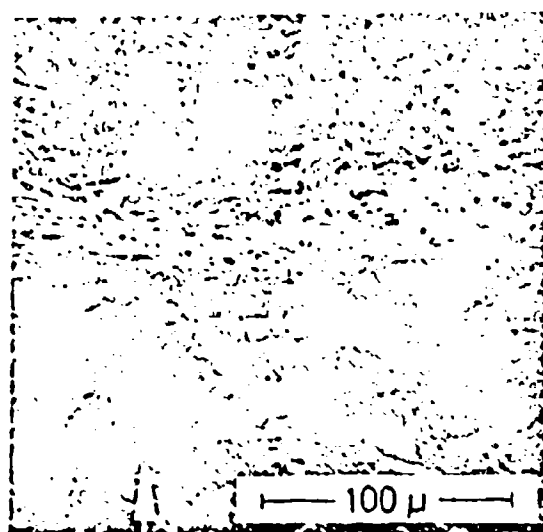


b)  $(dP/dt)_0 = 13 \times 10^3 \text{ atm/s}$  ( SAMPLE A-B )

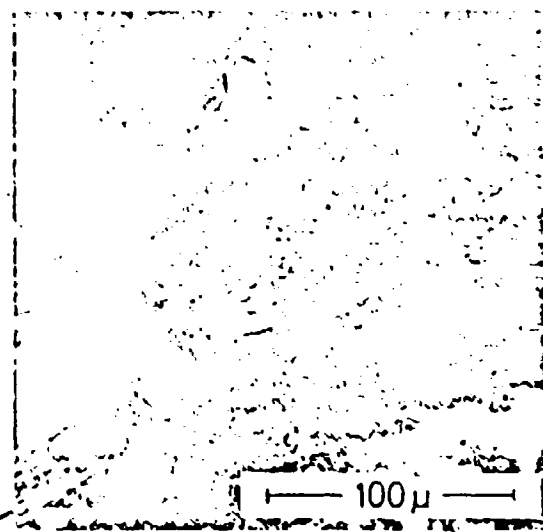


c)  $(dP/dt)_0 = 8,2 \times 10^3 \text{ atm/s}$  ( SAMPLE D )

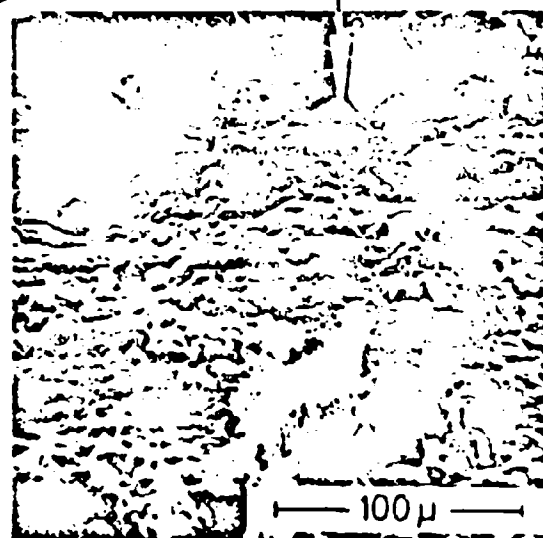
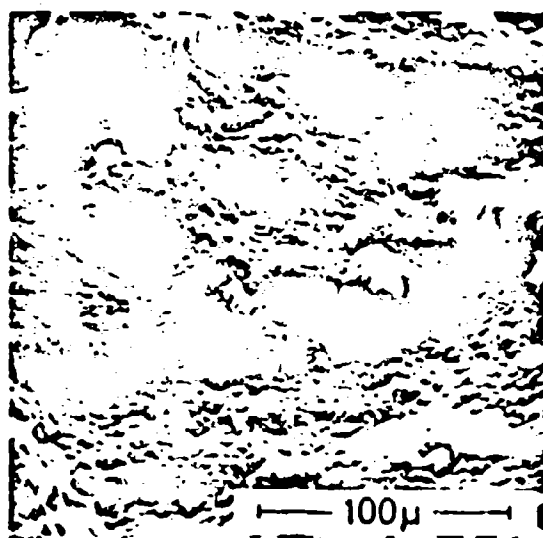
QUENCHED SURFACES FOR VARYING  $(dP/dt)_0$   
( 24% PBCT + 76% 25μ AP )



a)  $(dP/dt)_0 = 13 \times 10^3 \text{ atm/s}$   
( SAMPLE E )



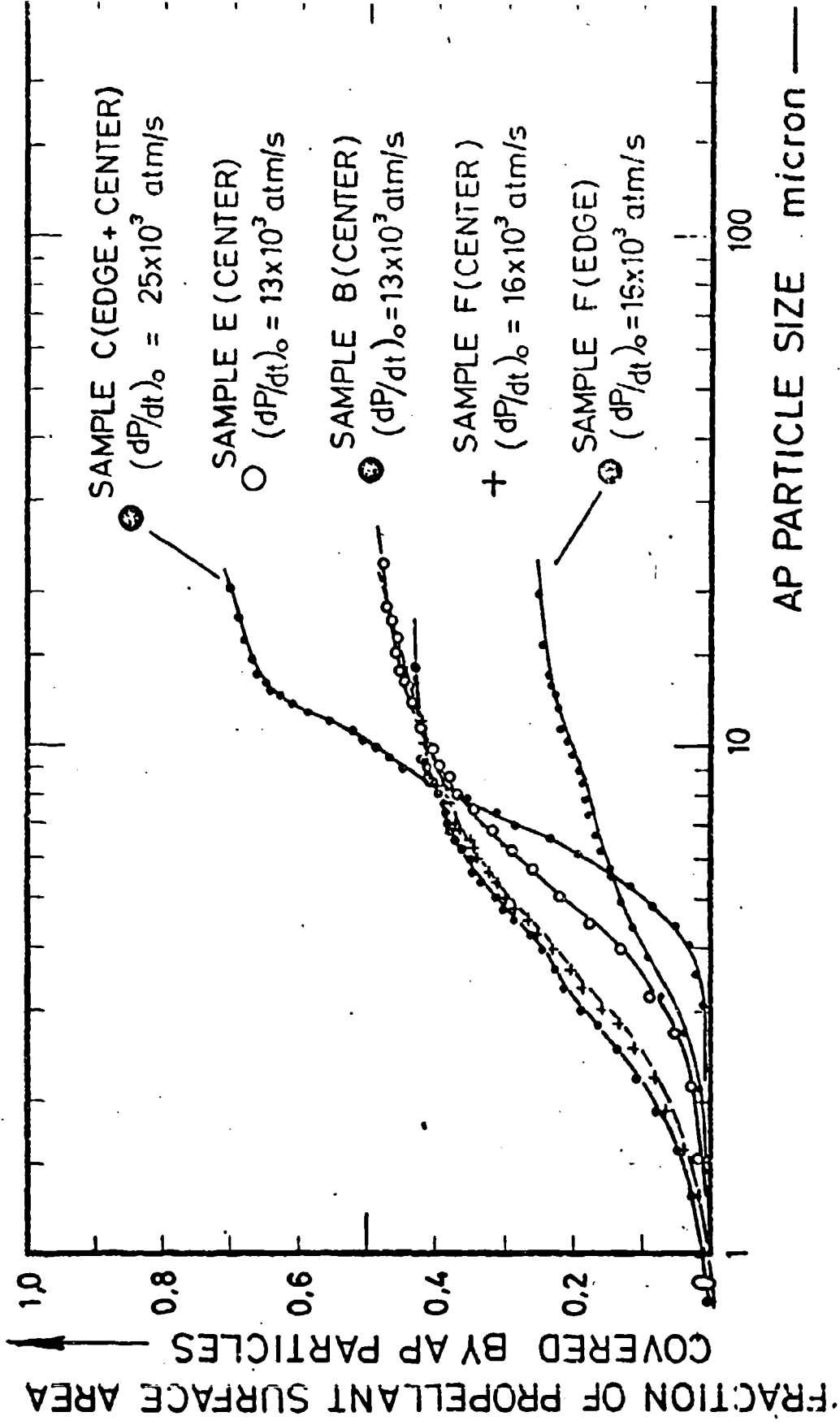
b)  $(dP/dt)_0 = 16 \times 10^3 \text{ atm/s}$   
( SAMPLE F )



Reproduced from  
best available copy.

SURFACE STRUCTURES AT MEDIUM  $(dP/dt)_0$   
( 24 % PBCT + 76 % 25 μ AP )





AP PARTICLE SIZE AND SURFACE COVERAGE FOR  
 FIG 9 EXTINGUISHED 24% PBCT + 75% 25 $\mu$  AP



a)  $(dP/dt)_0 = 19 \times 10^3 \text{ atm/s}$

Reproduced from  
best available copy.

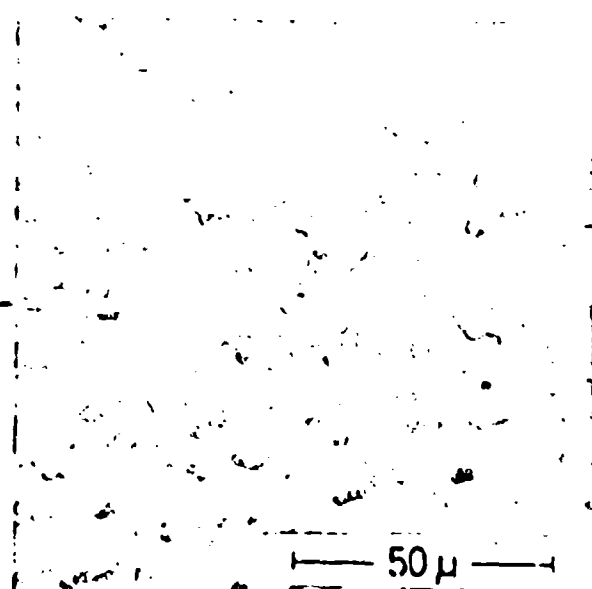
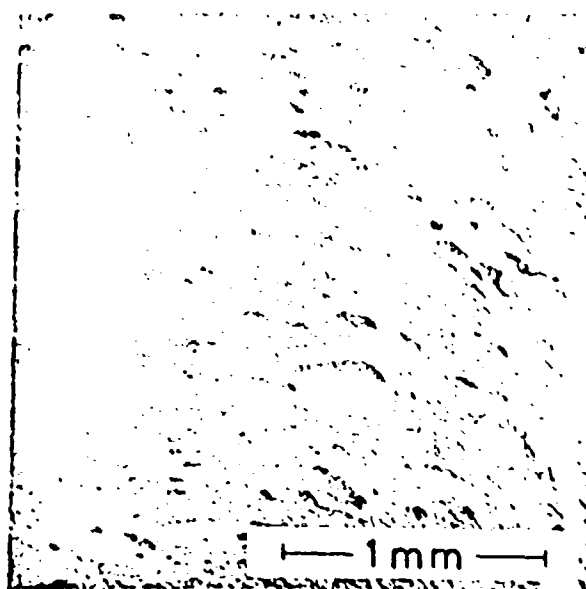


b)  $(dP/dt)_0 = 6,7 \times 10^3 \text{ atm/s}$

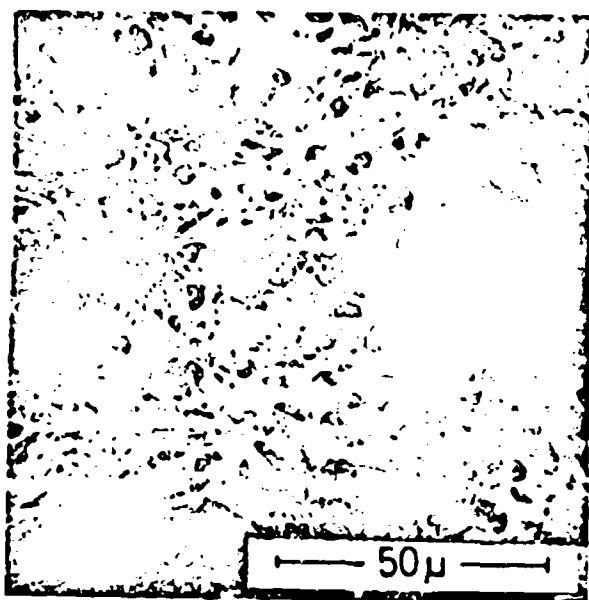
---

LARGE AP (200 $\mu$ ) PROPELLANTS QUENCHED  
WITH DIFFERENT  $(dP/dt)_0$   
( 24% PBCT + 76% AP )

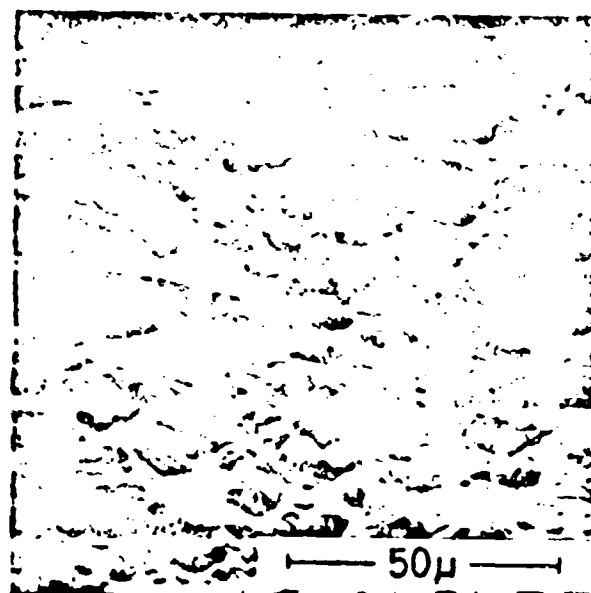
Fig 10



FLAME QUENCHED WITH  $N_2$  AT  $-190^\circ C$



PRE-HEATED  $N_2$

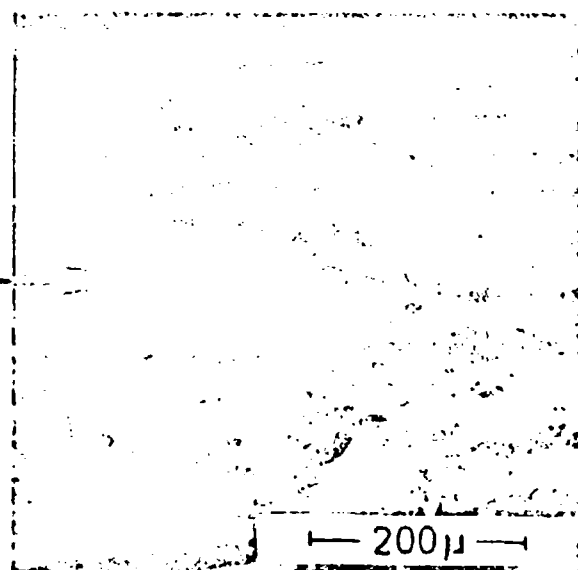
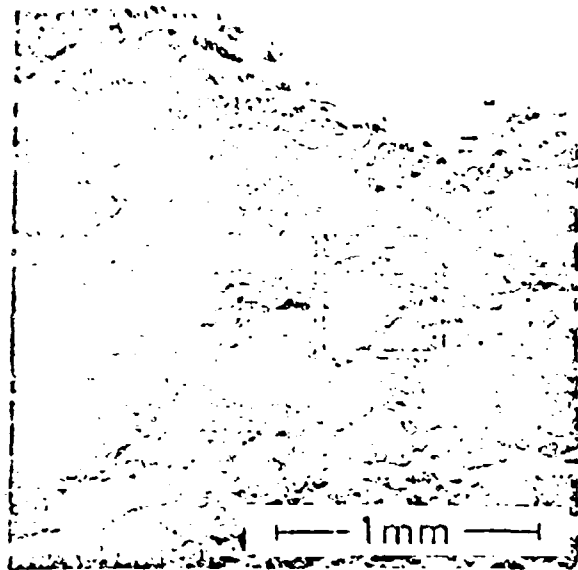


$N_2$  AT  $+20^\circ C$

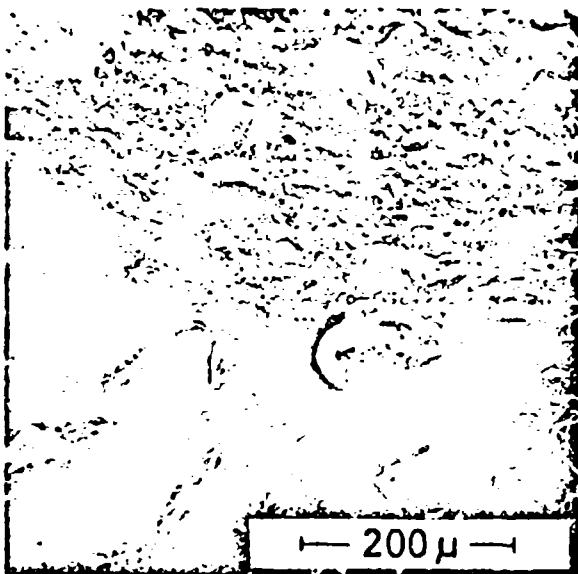
Reproduced from  
best available copy.

EFFECT OF  $N_2$  BLOWING TEMP. ON  
THE SURFACE STRUCTURE OF  
24% PBCT + 76%  $25\mu$  AP.

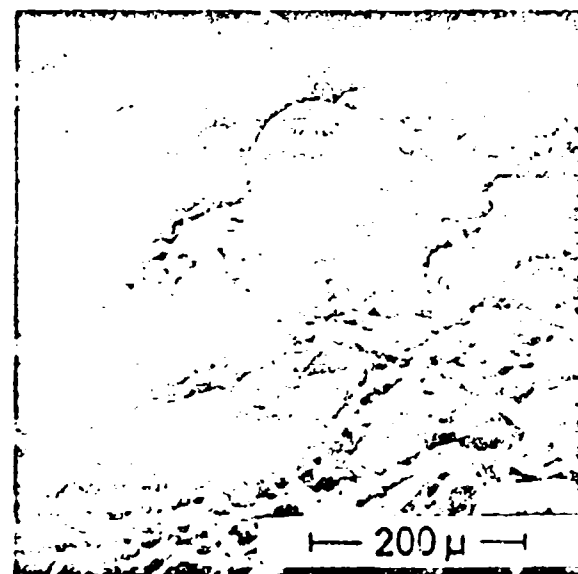
Fig 11



FLAME QUENCHED WITH  $N_2$  AT  $-190^\circ C$



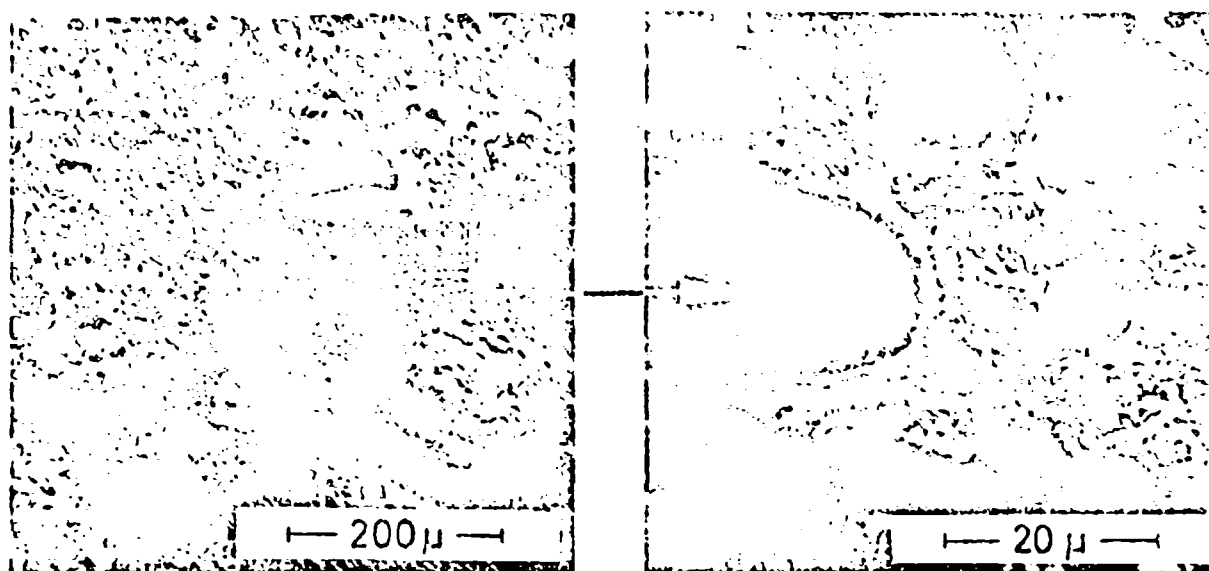
PREHEATED  $N_2$



$N_2$  AT  $+20^\circ C$

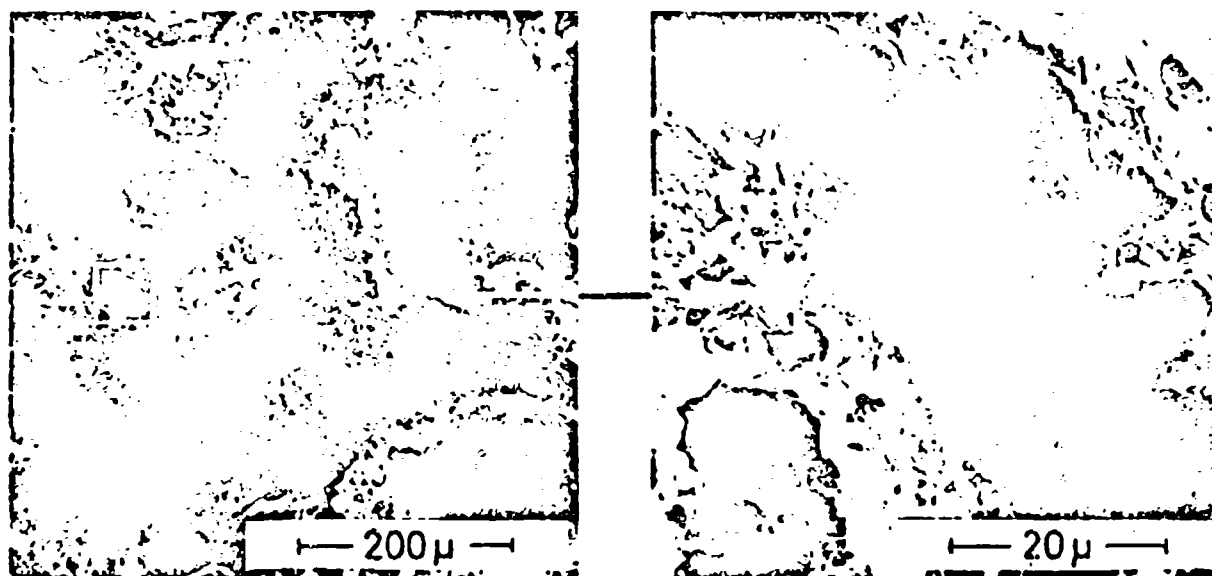
Reproduced from  
best available copy.

EFFECT OF  $N_2$  BLOWING TEMP. ON  
THE SURFACE STRUCTURE OF  
24% PBCT + 76% 200μ AP



20  $\mu$  AP PARTICLE SIZE ; 1 atm

Reproduced from  
best available copy.



200  $\mu$  AP PARTICLE SIZE ; 0,1 atm

---

SURFACE STRUCTURE OF PROPELLANT  
QUENCHED ON METAL PLATE  
(24% PBCT + 76% AP)

Key words:

Ammonium Perchlorate, Composite Propellant, Extinguishment, Repressurization, Transient Combustion, Flame, High Speed Film, Spectrography, Scanning Electron Microscope, Particle Size Distribution, Microstructure.

UNCLASSIFIED

Security Classification

DOCUMENT CONTROL DATA - R & D		
(Security classification of title, body of abstract and indexing annotation must be entered when the overall report is classified)		
1. ORIGINATING ACTIVITY (Corporate author) DEUTSCHE FORSCHUNGS-u. VERSUCHSANSTALT FUR LIFT-und RAUMFAHRT - INSTITUT FUR CHEMISCHE RAKETENANTRIEBE 3041 TRAUEN, WEST GERMANY		2a. REPORT SECURITY CLASSIFICATION UNCLASSIFIED
3. REPORT TITLE  DEPRESSURIZATION EXTINGUISHMENT OF COMPOSITE SOLID PROPELLANTS: FLAME STRUCTURE, SURFACE CHARACTERISTICS, AND RESTART CAPABILITY		2b. GROUP
4. DESCRIPTIVE NOTES (Type of report and inclusive dates) Scientific Final		
5. AUTHOR(S) (First name, middle initial, last name)  J A STEINZ H SELZER		
6. REPORT DATE Dec 1970	7a. TOTAL NO. OF PAGES 27	7b. NO. OF REFS 13
8a. CONTRACT OR GRANT NO  F61052-70-C-0013		5b. ORIGINATOR'S REPORT NUMBER(S)  5b. OTHER REPORT NUMBER(S) (any other numbers that may be assigned this report) <b>TR-72-1125</b>
a. PROJECT NO. 9711-01		
c. 61102F		
d. 681308		
10. DISTRIBUTION STATEMENT Approved for public release; distribution unlimited.		
11. SUPPLEMENTARY NOTES  TECH, OTHER		12. SPONSORING MILITARY ACTIVITY AF Office of Scientific Research (NAE) 1400 Wilson Boulevard Arlington, Virginia 22209
13. ABSTRACT During a rapid depressurization, the intensities of several spectral lines and the pressure are measured, simultaneous to the taking of high speed movie photographs of the flame. The end surfaces of all samples are analysed with a scanning electron microscope. BP + 76% 25µ AP propellant extinguishes permanently for initial depressurization rates exceeding ca. $7.5 \times 10^3$ atm/s, when the initial pressure is 45 atm. At the depressurization rates ( $16 \times 10^3$ atm/s), the gaseous flame quenches immediately due to the adiabatic expansion. Lower rates of fall in pressure ( $7 \times 10^3$ to $16 \times 10^3$ atm/s) allow a second flame to develop after 5 - 7 ms, the relaxation time of the solid phase. This new flame is irregular and partially consumes the AP particles available on the propellant surface, depending on the imposed dP/dt. The new flame goes out only at the end of the pressure transient. The restart capability of the propellant is most favorable when the imposed (dP/dt) <sub>0</sub> is considerable above (twice) that required for permanent extinction. The reduction of pressure is never an exponential function of time throughout the transient. Increased AP particle size of the propellant yields qualitatively similar results. Other methods of extinguishing a propellant flame give quenched surfaces with drastically different structural characteristics. The investigation shows that previous one-dimensional and/or linearized theories of propellant burning can not be valid for the phase where the new flame is developed.		

DD FORM 1473  
1 NOV 61

UNCLASSIFIED

Security Classification

UNCLASSIFIED

Security Classification

14 KEY WORDS	LINK A		LINK B		LINK C	
	ROLE	WT	ROLE	WT	ROLE	WT
AMMONIUM PERCHLORATE						
COMPOSITE PROPELLANT						
EXTINGUISHMENT						
DEPRESSURIZATION						
TRANSIENT COMBUSTION						
FLAME						
HIGH SPEED FILM						
SPECTROGRAPHY						
SCANNING ELECTRON MICROSCOPE						
PARTICLE SIZE DISTRIBUTION						
MICROSTRUCTURE						
IGNITION						

UNCLASSIFIED